https://doi.org/10.46813/2025-157-107

PULSED SOURCE OF TITANIUM, ZIRCONIUM AND OXYGEN PLASMAS MIXTURE FOR MAGNETOPLASMA SEPARATOR DIS-1

V.V. Katrechko[1], V.B. Yuferov[1], D.V. Vinnikov[1,2], V.I. Tkachev[1], A.N. Ozerov[1], I.N. Onishchenko[1], S.A. Petrenko[1], B.O. Brovkin[1]
[1]NSC "Kharkiv Institute of Physics and Technology", Kharkiv, Ukraine;
[2]O.Ya. Usikov Institute for Radiophysics and Electronics of the National Academy of Sciences of Ukraine, Kharkiv, Ukraine
E-mail: katrechko1609@gmail.com

The design and operational features of a new plasma source of the electric discharge type with zirconium (Zr) – titanium (Ti) electrodes and a zirconium oxide (ZrO) dielectric are analyzed in order to simulate the separation of 3 groups of Spent Nuclear Fuel – nuclear fuel and 2 groups of fission products with a mass ratio of 3:2:1. The plasma flux density at a voltage of 20 kV and a current of 10 kA, as well as the electron and ion currents for the simulant materials, were evaluated. The trajectories of FP ions in the crossed radial electric and longitudinal magnetic fields of the separator were calculated. The conditions necessary for achieving spatial ion separation by mass within the existing geometry of the separator chamber were determined: a radial electric field amplitude of E = 400 V/m and a longitudinal magnetic field of B = 0.4 T.

PACS: 28.41Kw, 52.50.Dg, 52.25.Jm

INTRODUCTION

In 2024, nuclear energy accounted for over 60% of electricity generation in Ukraine. Considering the challenges facing the country's energy sector and the specific characteristics of electricity production at nuclear power plants – such as the inability to rapidly adjust capacity to meet demand, making quick replacement with other sources unfeasible – it is critical to address the management of radioactive waste (RW) and spent nuclear fuel (SNF) produced during the operation of WWPR-1000 and other reactor types. These reactors utilize fuel elements composed of uranium dioxide (UO_2), a dielectric powder pressed into a specific shape. An urgent task is the separation of uranium dioxide (UO_2) and minor actinides (e.g., Pa, Th, Np) from radioactive waste, which requires proper disposal and poses significant environmental risks.

To explore this possibility, the concept of magnetoplasma processing was developed at the National Center of the KhPTI. This approach involves the use of crossed radial electric and longitudinal magnetic fields to initiate and control the spatial separation of ions by mass [1–3]. For research experiments, a coaxial electroerosion-type source operating in a frequency-pulse mode was identified as the optimal solution. These sources, often employed as plasma guns in accelerators – particularly those with inductive energy storage and plasma current switches – provide a pulse duration of up to 50 μs. This duration is sufficient for the effective operation of diagnostic tools such as Langmuir probes, current collectors, and spectroscopic instruments. Plasma guns of this type can generate plasma densities of up to 10^{16} cm^{-3} [4], and, with the inclusion of a nozzle, ensure axial symmetry of the plasma flow. Importantly, they are capable of using metals and metal oxides as the working medium.

To investigate the feasibility of implementing the magnetoplasma method, research should be focused on existing experimental setups and safe material simulants, such as Zr, Ti, and O. An additional advantage of using the frequency-pulse mode is the reduction of thermal load on the magnetic and electric field power supply systems, which are required to reach field strengths of up to 0.5 T and 400 V/m, respectively [5–9].

DESIGN AND FEATURES OF THE PLASMA SOURCE

Based on the conducted assessments, a plasma source was developed and manufactured, operating on the principle of pulsed discharge across the surface of a dielectric placed between coaxial electrodes. Materials simulating spent nuclear fuel were used for the electrodes and dielectric: zirconium was used to simulate U-238, titanium to simulate refractory metals (e.g., strontium), and oxygen to simulate volatile gases found in spent fuel, such as helium and oxygen. Structurally, the plasma source consists of:

- Zirconium cylinder – the outer electrode of the anode (Zr).
- Titanium rod – the inner electrode of the cathode (Ti).
- A dielectric ring of zirconium dioxide, which is located between the electrodes (ZrO_2).

The discharge occurs along the surface of zirconium oxide, resulting in the ejection of both the dielectric material and the electrode material into the surrounding space. Drawings and photographs of the plasma source are presented in Figs. 1 and 2. It is important to note that surface discharges on ceramic dielectrics (particularly ferroelectric ceramics) have been extensively studied in the high-energy range (U discharge > 100 kV), where a high dielectric constant (ε) ensures higher breakdown voltages. Such systems are utilized in applications requiring the generation of heavy ions (e.g., Pb, Zr, Ti) compared to traditional plasma guns that primarily operate with lighter elements such as C, H, and F.

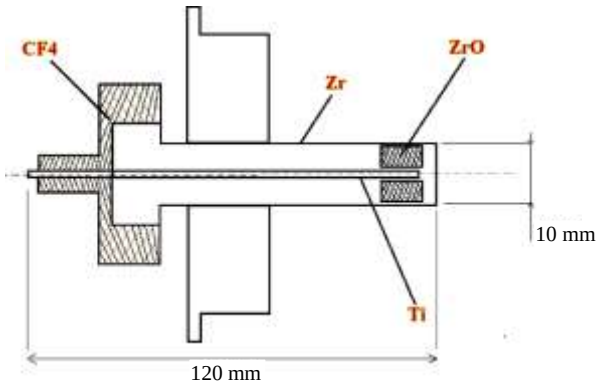

Fig. 1. Drawing of the plasma source of the magnetoplasma separator DIS-1

Table presents the components of the electrodes and the dielectric used in the plasma source, along with their ionization potentials. As observed, by creating a low-temperature plasma (Te < 10 eV), it can be expected that the plasma will primarily contain singly charged ions, which will not significantly influence the spatial distribution of plasma flows within the evacuated chamber of the magnetoplasma separator. A notable advantage of using plasma generated from metals and metal oxides is the absence of recycling processes, which are characteristic of gas plasmas. Recycling occurs when gas ions, after etching a surface, are not deposited as a film but are instead etched back into the plasma flow, leading to energy losses due to recharging and recombination processes

a

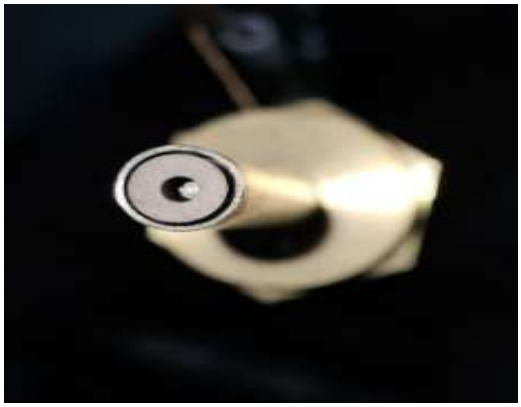

b

Fig. 2. Photographs of a plasma source with electrodes in the form of spent fuel simulant materials (a – general view, b – photo of the end surface)

Energy characteristics of plasma source ions

Components and their ionization potentials	1, eV	2, eV	3, eV	Dissociation, eV
ZrO	6.81	–	–	7.33
Zr	6.84	13.13	22.99	–
Ti	6.82	13.58	27.49	–
O	13.6	35.11	54.9	–

CHARACTERISTICS OF THE DISCHARGE AND THE DISCHARGE CIRCUIT

As noted, coaxial plasma sources operating in pulsed mode are capable of generating plasma with a density of $10^{12}…10^{1}$ cm^{-3}. Combined with the ability to use metals and metal oxides as working substances, this provides a significant advantage over stationary sources based on arc discharge, reflection discharge, and similar methods. Studies [10, 11] indicate that for an effective separation process, it is desirable to achieve a plasma density of 10^{13} cm^{-3} in the plasma source zone and 10^{11} cm^{-3} in the spatial separation zone, where heavy ions are directed toward the side surface of the chamber.

To power the plasma source, a high-voltage circuit comprising an URS-70 transformer and an IK-100-0.3 capacitor was employed. The charging circuit enables plasma discharges at voltages up to 25 kV with a pulse repetition rate of up to 1 Hz [12]. The plasma source demonstrated successful performance in terms of electroerosion resistance and stability of electrophysical parameters during research experiments at operating voltages ranging from 10 to 25 kV.

Fig. 3 presents a typical oscillogram of the plasma source current recorded at a charging voltage of U = 14.5 kV. The maximum current reaches 6 kA, with a pulse period of 5.3 μs and a duration of approximately 40 μs. In this operating mode, the plasma source underwent successful testing, with operational characteristics monitored over 1500 pulses at a frequency of 1…2 Hz.

Fig. 4 shows a frame-by-frame scan of the discharge with a period of 1 ms, recorded using a Casio Exilim EX-FH100 Black high-speed video camera operating at a frame rate of f = 1000 fps. As observed, following the formation of the main plasma jet, the area near the source remains illuminated for 1…2 ms. This glow is attributed to pre-ionization processes, during which an electron transitions to another orbit, emitting light in the form of photons. These processes have a duration of several milliseconds, which is 1–2 orders of magnitude longer than the discharge current duration of the plasma source.

To monitor the erosion of source materials, a polished stainless steel target was installed. After 200 discharges, a Zr and Ti film with a thickness of several nanometers was detected on the target, confirming the absence of a droplet phase during the discharge.

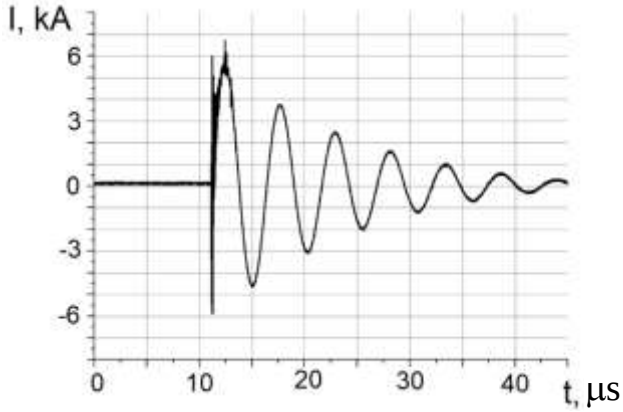

Fig. 3. Typical oscillogram of the discharge pulse of the plasma source current at a charging voltage of 14.5 kV

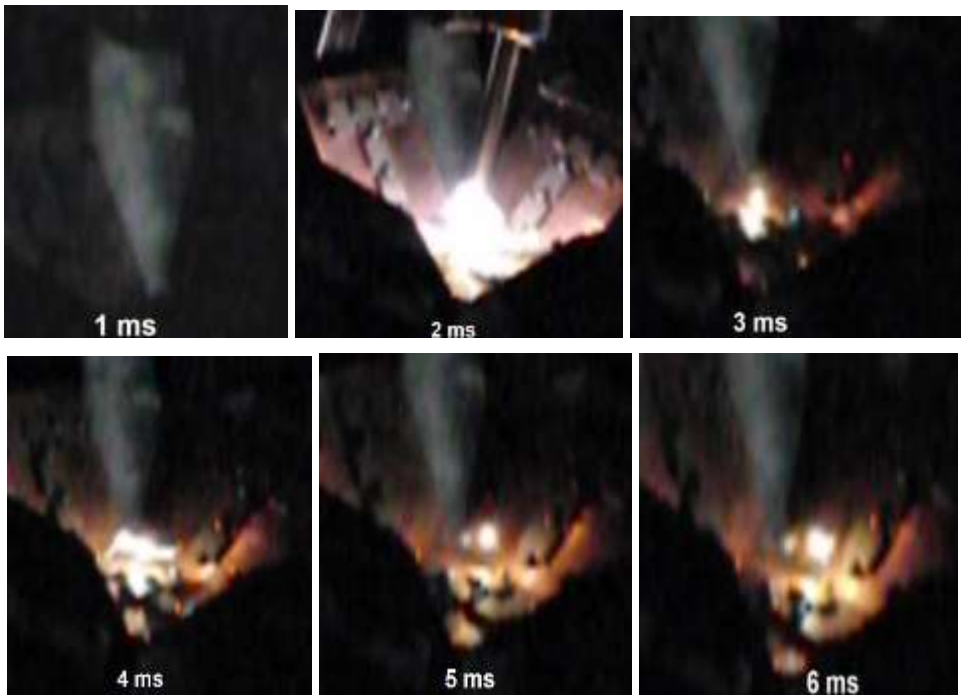

Fig. 4. Frame-by-frame scan of the discharge flow of the pulsed plasma source of the magnetoplasma separator DIS-1

To estimate the density of the discharge plasma generated by the source, Ampere's law is applied, which relates the current density to the plasma characteristics, given the known surface area of the dielectric and the maximum current (Equation 1):

$$J = n_e * e * v_d, \quad (1)$$

where j – current density on the dielectric surface (A\m^2); n_e – electron density; e – electron charge; v_d – drift velocity of plasma electrons. $vd=(2\cdot k_B\cdot T/m_e)^{1/2}$; k_B – Boltzmann constant; T – plasma temperature.

The dielectric surface area reaches 48.7 mm^2. The current density, taking into account the current of 6 kA, reaches $j \sim 1.05\cdot10^8$ A/m^2. The drift velocity of electrons, taking into account the plasma temperature of 5 eV, is v_d ~$1.3\cdot10^6$ m/s. Expressing ne from equation (1) and substituting the parameters calculated above, we obtain the estimated plasma electron density: $n_e = 5 \sim 10^{14}$ cm^{-3}.

To estimate the electron and ion currents of the plasma source components in a flat geometry and under a longitudinal magnetic field, without accounting for collisions, the Child-Langmuir equation can be applied. Equation (2) describes the electron current, while Equation (3) represents the ion current [13]:

$$J_e[A/cm^2] = \frac{\sqrt{2}}{9\pi}\cdot\frac{\sqrt{e\cdot U^3}}{\sqrt{m_e}\cdot d^2} = 2.33\cdot10^{-6}\frac{\sqrt{U^3}}{d^2},$$

$$J_e[A/cm^2] = \frac{\sqrt{2}}{9\pi}\cdot\frac{\sqrt{e\cdot U^3}}{\sqrt{m_e}\cdot d^2} = 2.33\cdot10^{-6}\frac{\sqrt{U^3}}{d^2}, \quad (2)$$

$$J_{z+}[A/cm^2] = \frac{\sqrt{2}}{9\pi} \cdot \frac{\sqrt{e \cdot U^3}}{\sqrt{m_z} \cdot d^2} = 5.46 \cdot 10^{-8} \frac{\sqrt{U^3}}{\sqrt{m_z} \cdot d^2},$$

$$J_{z+}[A/cm^2] = \frac{\sqrt{2}}{9\pi} \cdot \frac{\sqrt{e \cdot U^3}}{\sqrt{m_z} \cdot d^2} = 5.46 \cdot 10^{-8} \frac{\sqrt{U^3}}{\sqrt{m_z} \cdot d^2}, \quad (3)$$

where e – charge of an electron; me – mass of an electron (me = 1/1836 m_H^+); m_H^+ – mass of a hydrogen ion; m_z+ – mass of the target ion; J_e – electron current; J_z^+ – ion current; d – distance of the anode-cathode gap; U – voltage.

For calculations, we take into account the emission area of the side surface of the collector zone of the evacuated separator chamber (10^3 cm^{-3}) and the achievable values of the radial electric field strength (up to 1000 V/m). he results of these calculations are presented in the graphs of Fig. 5.

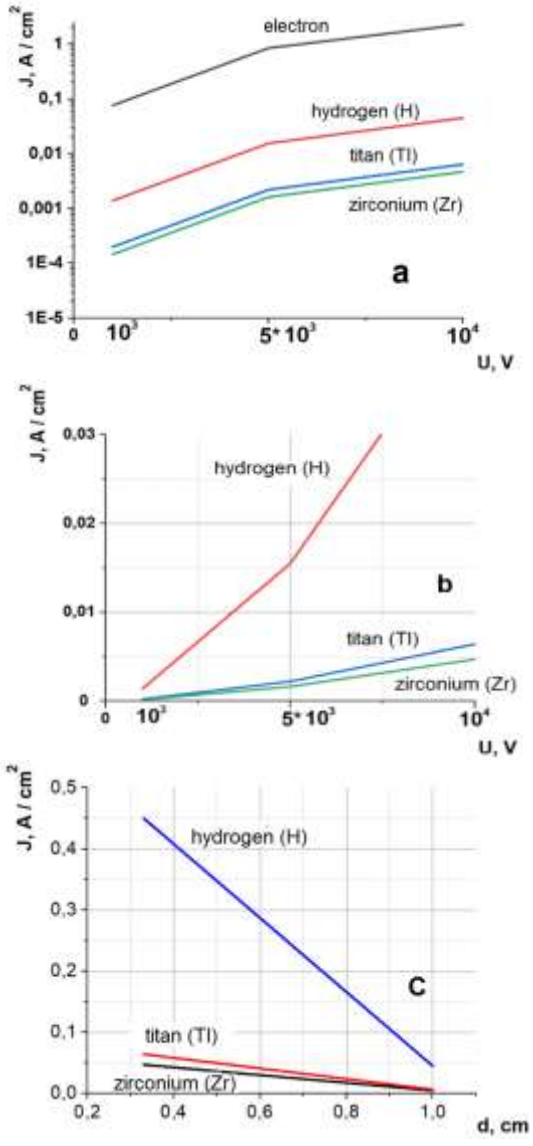

Fig. 5. Graphs of the density of ion and electron currents of the source plasma depending on the voltage across the gap and its length (a – for electrons and ions depending on the voltage; b – for ions depending on the voltage; c – for ions depending on the length of the gap)

For comparison, the hydrogen ion is used as a reference. Estimates indicate that the available parameters of the source and separator systems enable the extraction of an ion current of approximately 20 A for target zirconium ions with a mass of M=91.

CALCULATIONS OF THE ELECTROMAGNETIC FIELD AND INITIAL ENERGIES FOR SPATIAL SEPARATION OF TARGET IONS

The concept of magnetoplasma material separation involves a sequence of stages: crushing [14], heating, ionization, and separation in crossed electromagnetic fields. During the final stage, the plasma rotates within radial electric and longitudinal magnetic fields. In this process, ions with greater mass acquire transverse energy and radial velocity more rapidly, leading to their deposition on the lateral surface. Conversely, ions with smaller masses follow cycloidal trajectories in the longitudinal direction, accompanied by magnetized electrons, and are deposited on the end surface.

The radial electric field of the separator is generated using eight coaxial tungsten electrodes positioned inside the evacuated chamber. The smallest ring has a diameter of 2.5 cm, while the largest measures 14 cm. This system functions as a plasma mass filter, where the highest potential is located along the axis of the chamber (in contrast to a centrifuge, where the potential is highest at the periphery). A potential ranging from 40 to 140 V is applied to the electrodes.

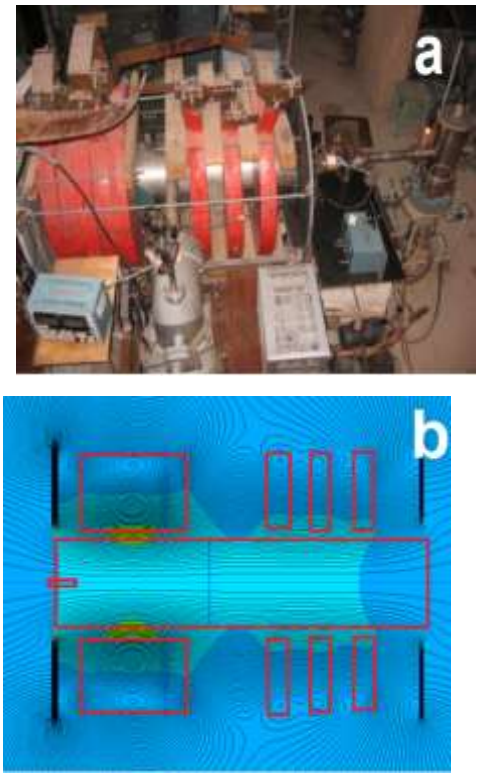

Fig. 6. General photograph of the magnetoplasma separator with the location of the magnetic field solenoids (a), and the topography of the magnetic field at a current in the windings of 100 A (equivalent B = 0.12 T) (b)

The longitudinal magnetic field of the separator is created by a system of eight solenoids positioned outside the evacuated stainless steel chamber. These

solenoids generate a stationary magnetic field with an amplitude of up to 0.5 T (Fig. 6).

The plasma of the simulant materials in the magnetoplasma separator is a multicomponent mixture. In addition to the primary components produced by the electroerosion and sublimation of the electrodes and source dielectric (Zr, Ti, O, ZrO), it includes residual gases and other elements not directly related to the research objectives (e.g., H, N, N, C). This composition partially replicates the structure of non-radioactive spent fuel, known as SIMFUEL, produced under laboratory conditions for further experimental studies [15, 16].

In crossed radial electric (E) and longitudinal magnetic (H) fields, two primary forces act on a particle: the Lorentz force and the centrifugal force, which arises from rotation around a specific axis. The force balance for the plasma mass filter is described by the following equation [17, 18].

Fig. 7 presents the calculated graphs of the ion trajectories from the plasma source within the evacuated chamber of the magnetoplasma separator. The calculations were performed for varying amplitudes of the stationary magnetic field and different initial ion energies (the energy acquired by the ions during ionization in the plasma source) at E=400 V/m.

Calculations indicate that for a more controlled separation process, with the spatial separation of target Zr ions simulating nuclear fuel ions in spent fuel, it is advisable to generate plasma with an energy exceeding 30 eV. Under these conditions, the target ions are deposited onto the side surface of the separator chamber over a length of 90…105 cm. To ensure effective operation with low-temperature plasma and to prevent a decrease in system efficiency, it is recommended to increase the amplitude of the magnetic field to 0.4…0.5 T.

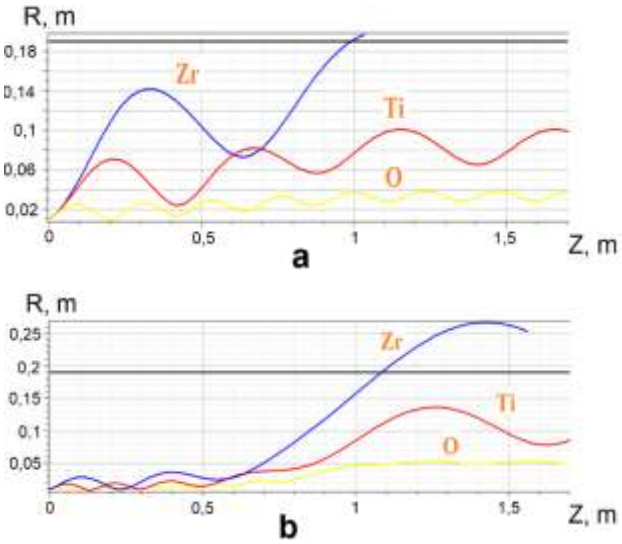

Fig. 7. Trajectories of plasma ions in the DIS-1 magnetoplasma separator (a – initial particle energy – 35 eV, magnetic field amplitude – B = 0.13 T; b – initial particle energy – 12 eV, magnetic field amplitude – B = 0.4 T)

CONCLUSIONS

In the Department of Small-Size Accelerators and Separation Technologies at NSC KIPT, a plasma jet of the electroerosion type was developed using NSF simulants as the working material. The new source offers several advantages, including the ability to work with plasma composed of metals and metal oxides, the occurrence of recycling processes from the vacuum chamber walls with corresponding additional energy consumption, and an increase in plasma density up to 10^{14} cm^{-3}. Thermal overheating resulting from the pulsed mode of operation is also a notable feature.

The source ensures a maximum electron and ion flow for Zr and Ti ions of approximately 20 A. The optimal electromagnetic field parameters (amplitude values) and core energies required for the spatial separation of plasma ions have been determined. It is possible to isolate specific ion groups at magnetic field amplitudes of B=0.4 T and electric field strengths of up to E=400 V/m within a controlled area, given an initial ion energy of 10…12 eV.

REFERENCES

1. V.B. Yuferov et al. Magnetoplasma regeneration of spent nuclear fuel // *Bulletin of the National Technical University "KhPI": collection of scientific papers. Thematic issue: Problems of improving electrical machines and devices*. Kharkiv: NTU “KhPI”, 2010, No. 55, p. 129-149.

2. V.B. Yuferov, O.M. Yegorov, V.O. Ilyichova, S.V. Shariy, K.I. Zhivankov. Plasma separation of waste products is one of the possible ways to solve the problem of a closed nuclear fuel cycle // *Problems of Atomic Science and Technology*. 2013, No 2(84).

3. V.B. Yuferov, O.M. Yegorov, V.O. Ilyichova, S.V. Shariy, K.I. Zhivankov. Plasma separation of wastes – one of the possible ways to solve the problem of a closed nuclear fuel cycle // *Problems of Atomic Science and Technology*. 2013, No 2(84).

4. US Patent №6096220. Plasma Mass Filter/Tihiro Ohkawa // Fil. 16.11.1998. Publ. 01.08.2000. 3. Band gap plasma mass filter. EP 1 351 273 A1 Date of publication: 08.10.2003 Bulletin 2003/41.

5. W.H. Bostick. Experimental Study of Ionized Matter Projected Across a Magnetic Field // *Physical Review*. 1956, v. 104(2), p. 292-299.

6. S.K. Zhdanov, V.A. Kurnaev, M.K. Romanovsky, I.V. Tsvetkov. *Fundamentals of physical processes in plasma and plasma accelerators* / Ed. by V.A. Kurnaev. M.: “MEPhI”, 2007, 368 p.

7. V.B. Yuferov, E.I. Skibenko, V.I. Tkachov, V.V. Katrechko, A.S. Svichkar. The atomic molecular processes in a hydrogen plasma at initial stage of a discharge // *Problems of Atomic Science and Technology. Series “Plasma Electronics and New Methods of Acceleration*”. 2019, No 4, p. 105-109.

8. V.B. Yuferov, S.V. Katrechko, V.O. Ilichova, S.V. Shariy, A.S. Svichkar, M.O. Shvets, E.V. Mufel, A.G. Bobrov. Developing the Concept of Multi-Stage Spent Fuel Cleaning From fission Products by Physical Methods // *Problems of Atomic Science and Technology*. 2018, No 1, p. 118-126.

9. V.B. Yuferov, A.S. Svichkar, V.V. Katrechko, T.I. Tkachova, S.V. Shariy, V.O. Ilichova. Comparative Characteristics of Atomic and Molecular Plasma in Stationary and Pulsed Discharges // *Problems of Atomic Science and Technology*. 2015, No 6(100).

10. V.B. Yuferov, A.S. Svichkar, S.V. Shariy, V.V. Katrechko, T.I. Tkachova. Dynamics ion flows in a rotating plasma // *East Eur. J. Phys*. 2014, v. 1, No 2, p. 96-99.

11. V.V. Katrechko, V.B. Yuferov, V.O. Ilichova, S.N. Khizhnyak. Spatial Separation of the Ions of a Given Mass Range in the Demo-Imitation Separator at the First Turn of Ionic Trajectory // *Problems of Atomic Science and Technology*. 2021, No 4(134).

12. V.B. Yuferov, V.V. Katrechko, D.V. Vinnikov, V.I. Tkachev, D.D. Sorokina. On some features of magnetic systems for plasma processing of spent nuclear fuel (SNF) // *Problems of Atomic Science and Technology*. 2022, No 4(140).

13. D.V. Vinnikov, V.V. Katrechko, V.B. Yuferov, V.I. Tkachev. Plasma Guns of an Erosion Type with the Pulse-Periodic Gas-Metal Injection // *Problems of Atomic Science and Technology*. 2022, No 6(142), p. 60-65. https://doi.org/10.46813/2022-142-060

14. A.S. Fedorov. General solution of the Bursian problem // *Technical Physics.* 2011, v. 56, p. 1406-1413.

15. D.V. Vinnikov, V.V. Katrechko, N.A. Shulgin, V.B. Yuferov, V.I. Sokolenko, V.I. Tkachev, A.N. Ponomarev, I.V. Buravilov. Grinding of materials simulating spent nuclear fuel for magnetoplasma separation // *Problems of Atomic Science and Technology*. *Series "Physics of Radiation Effect and Radiation Materials Science*". 2016, No 4(104), p. 54-57. doi:10.46813/2020-125-191

16. Niko Kivel, Natalia Shcherbina, Ines Gunter Leopold. Development of a high temperature treatement device for spent nuclear fuel // *J. Radioanal Nucl. Chem.* DOI 10.1007|s 10967-012-2046-x

17. J. Svedkauskaite-Le Gore, N. Kivel, J.J. Gunter-Leopold. Real time measurement of fission products released from spent fuel by thermal treatment // *J. Radioanal Nucl. Chem*. DOI 10.1007|s 10967-012-2046-x. 25. T

18. R.L Miller, T.R. Jarboe, M.V. Sadowski, and U. Shumlak. Plasma mass filter for separating radioactive waste. Nuclear Instruments and Methods in Physics Research Section A: Accelerators, Spectrometers // *Detectors and Associated Equipment*. 2008, v. 595(3), p. 334-341.

19. V.B. Yuferov, E.I. Skibenko, I.V. Buravilov, A.S. Svichkar, A.N. Ponamoriev, V.V. Katrechko, V.V. Nikulshina. Small-Size "DI-2" Accelerator with the Plasma Current Switch and Inductive Energy Accumulator as a Material Irradiation Test Rig // *Problems of Atomic Science and Technology*. 2022, No 4(140), p. 154-156. https://doi.org/10.46813/2022-140-154.

Article received 14.04.2025

ІМПУЛЬСНЕ ДЖЕРЕЛО СУМІШІ ПЛАЗМИ ТИТАНУ, ЦИРКОНІЮ І КИСНЮ ДЛЯ МАГНІТОПЛАЗМОВОГО СЕПАРАТОРА ДИС-1

В.В. Катречко, В.Б. Юферов, Д.В. Вінніков, В.І. Ткачов, А.Н. Озеров, І.М. Оніщенко, С.О. Петренко, Б.О. Бровкін

Розглянуто конструкцію та особливості роботи нового джерела плазми електророзрядного типу з електродами цирконій (Zr) – титан (Ti) і діелектриком – оксид цирконію (ZrO). Проведено оцінку густини плазмового потоку при напрузі 20 кВ і струмі 10 кА, а також електронного та іонного струмів для матеріалів-імітаторів. Розраховано траєкторії іонів у схрещених радіальному електричному та поздовжньому магнітних полях сепаратора. Знайдено умови, за яких можна досягти просторового розділення іонів за масою при існуючій геометрії камери сепаратора: амплітуда радіального електричного поля E=400 В/м і поздовжнє магнітне поле B=0,4 Тл.